Electrochimica Acta 125 (2014) 497–502

Contents lists available at ScienceDirect

Electrochimica Acta

journal homepage: www.elsevier.com/locate/electacta

Protective organic additives for high voltage $LiNi_{0.5}Mn_{1.5}O_4$ cathode materials

Seo-Youn Bae, Won-Kyung Shin, Dong-Won Kim*

Department of Chemical Engineering, Hanyang University, Seungdong-Gu, Seoul 133-791, Republic of Korea

ARTICLE INFO

Article history:
Received 14 November 2013
Received in revised form
31 December 2013
Accepted 20 January 2014
Available online 4 February 2014

Keywords:
Ionic liquid
Spinel $LiNi_{0.5}Mn_{1.5}O_4$
Organic additives
Solid electrolyte interphase

ABSTRACT

Dimethylacetamide (DMAc) and triethyl(2-methoxyethyl)phosphonium bis(trifluoromethylsulfonyl) imide (TEMEP-TFSI) are investigated as protective additives for high voltage $LiNi_{0.5}Mn_{1.5}O_4$ cathode materials. The capacity retention of Li/$LiNi_{0.5}Mn_{1.5}O_4$ cells is improved by adding these additives to the base liquid electrolyte. The self-extinguishing time and DSC results demonstrate that the addition of TEMEP-TFSI to the base electrolyte is effective in reducing the flammability of the electrolyte solution and improving the thermal stability of the $LiNi_{0.5}Mn_{1.5}O_4$ electrode. TEM and XPS analyses of the $LiNi_{0.5}Mn_{1.5}O_4$ electrode reveal that DMAc and TEMEP-TFSI participate in the formation of a stable solid electrolyte interphase (SEI) on the $LiNi_{0.5}Mn_{1.5}O_4$ electrode, and the resulting SEI layer effectively suppresses electrolyte decomposition.

1. Introduction

Spinel $LiMn_{1.5}Ni_{0.5}O_4$ cathode materials have been studied as a substitute for $LiCoO_2$ in lithium-ion batteries because of the economic and environmental advantages [1–3], and their high working voltage can produce a higher energy density than other cathode materials. However, the practical application of $LiMn_{1.5}Ni_{0.5}O_4$ materials to lithium-ion batteries is still challenging because they suffer from the oxidative decomposition of electrolyte solutions at high voltages, leading to the gradual deterioration of cell performance upon cycling. Numerous possible solutions to this problem have been proposed, such as the development of new electrolytes exhibiting high anodic stability [4,5], addition of various inorganic and organic additives to the electrolyte [6–11], and a polymer or inorganic coating on the surface of cathode materials [12–14]. Among various additives, a Lewis base, such as dimethylacetamide (DMAc), has been recognized as an effective stabilizing additive for active cathode materials by inhibiting reactions of the electrolyte with electrode materials [15,16]. Ionic liquids (ILs) have also been considered safe electrolyte additives due to their unique properties such as non-flammability and enhanced thermal stability [17–19]. Tsunashima and Sugiya reported that ILs based on triethylalkyl phosphonium cations with a bis(trifluoromethylsulfonyl) imide anion exhibited good electrochemical properties and high thermal stability [20].

In this work, DMAc and triethyl(2-methoxyethyl)phosphonium bis(trifluoromethylsulfonyl)imide (TEMEP-TFSI) were used as protective additives for high voltage $LiNi_{0.5}Mn_{1.5}O_4$ cathode materials. The cycling performance and thermal stability of the $LiNi_{0.5}Mn_{1.5}O_4$ electrodes were improved by introducing these additives to the base electrolyte through the formation of the protective surface layer. The surface layer formed on the electrodes during cycling was investigated by X-ray photoelectron spectroscopy (XPS).

2. Experimental

2.1. Cell assembly

DMAc (99.8%) was purchased from Sigma Aldrich and stored over 4 Å molecular sieves before use. TEMEP-TFSI was purchased from Nippon Chemical Industrial Co. Ltd. and dried under vacuum at 120 °C for 12 h before use. The water content in TEMEP-TFSI after drying was less than 20 ppm by Karl Fischer titration. The base electrolyte, 1.15 M $LiPF_6$ in ethylene carbonate (EC)/diethyl carbonate (DEC) (3:7 by volume, battery grade), was kindly supplied by Soulbrain Co. Ltd. and used without further treatment. In an Ar-filled glove box, 1 wt.% DMAc and 10 wt.% TEMEP-TFSI were directly added to the base electrolyte. Table 1 lists three different electrolyte systems considered in this study. The positive electrode was prepared by coating an N-methyl pyrrolidone (NMP)-based slurry containing 85 wt.% $LiMn_{1.5}Ni_{0.5}O_4$ (Samsung SDI), 7.5 wt.% poly(vinylidienefluoride) (PVdF) and 7.5 wt.% super-P carbon (MMM Co.) onto aluminum foil. The active mass loading corresponded to a capacity of 1.0 mAh cm^{-2}. The negative

* Corresponding author. Tel.: +82 2 2220 2337, fax: +82 2 2298 4101.
E-mail address: dongwonkim@hanyang.ac.kr (D.-W. Kim).

0013-4686/$ – see front matter © 2014 Elsevier Ltd. All rights reserved.
http://dx.doi.org/10.1016/j.electacta.2014.01.124

Table 1
Electrolyte systems considered in this study.

Electrolyte	Composition
E0	1.15 M $LiPF_6$ EC/DEC
E1	M $LiPF_6$ EC/DEC + 1 wt.% DMAc
E2	1.15 M $LiPF_6$ EC/DEC + 1 wt.% DMAc + 10 wt.% TEMEP-TFSI

electrode consisted of a lithium metal (Honjo Metal Co. Ltd., 100 m) that was pressed onto a copper current collector. In order to improve the wettability of the polyethylene separator for the electrolyte solution, a porous poly(vinylidenefluoride-co-hexafluoropropylene)-coated separator was prepared according to a procedure reported previously [21]. The CR2032-type coin cell composed of a lithium negative electrode, a polymer-coated separator and a $LiMn_{1.5}Ni_{0.5}O_4$ positive electrode was assembled with an electrolyte solution. All cells were assembled in a dry box filled with argon gas. After assembly, the cells were kept at 25 °C for 12 h to imbue the electrodes with the electrolyte solution.

2.2. Measurements

The conductivity measurements of the electrolyte solutions were performed using a Cond 3210 conductivity meter (WTW GmbH, Germany). The self-extinguishing time (SET) was measured to quantify the flammability of the electrolyte solutions, as previously described [22–24]. The cycling performance of $Li/LiMn_{1.5}Ni_{0.5}O_4$ cells was evaluated over a voltage range of 3.0–4.9 V at a 0.5 C rate and 25 °C with battery testing equipment (WBCS 3000, Wonatech). AC impedance measurements of the $Li/LiMn_{1.5}Ni_{0.5}O_4$ cells were performed at charged state (4.9 V) using a Zahner Electrik IM6 impedance analyzer over the frequency range of 1 mHz to 100 kHz with an amplitude of 10 mV. The surface morphology of the $LiNi_{0.5}Mn_{1.5}O_4$ particles after 100 cycles was observed using transmission electron microscopy (TEM, JEM 2100F, JEOL). Surface characterization of the $LiNi_{0.5}Mn_{1.5}O_4$ electrodes before and after cycling in different electrolyte systems was conducted by XPS. The electrodes were washed several times with anhydrous DMC to remove residual electrolyte, followed by vacuum drying overnight at room temperature prior to collecting the data. The electrodes were transferred in an air-tight container, mounted on the XPS sample holder and transferred to the XPS apparatus with minimal exposure to air. XPS measurements were conducted on a VG Multilab ESCA 2000 system using an Al Kα radiation. For the differential scanning calorimetry (DSC) measurements of the delithiated $Li_{1-x}Ni_{0.5}Mn_{1.5}O_4$ materials, the cells were fully charged to 4.9 V after 100 cycles and were disassembled in a dry room. The cathode materials scraped from the current collector were rinsed with DMC to remove the residual electrolyte and dried under vacuum. The electrodes were sealed together with the electrolyte solution in a hermetic stainless steel pan, and measurements were performed at a heating rate of 5 °C min^{-1}. A 30 wt.% electrolyte solution was used based on the active cathode material, and the heat flow was calculated based on the weight of the active cathode material.

3. Results and discussion

Fig. 1 shows the ionic conductivities of the base electrolyte (E0) and electrolyte solutions containing different additives (E1, E2). The ionic conductivity of the base electrolyte was 6.8×10^{-3} S cm^{-1}. When 1 wt.% DMAc was added to the base electrolyte, the ionic conductivity was scarcely changed. On the other hand, the electrolyte solution containing 1 wt.% DMAc and 10 wt.% TEMEP-TFSI showed a slightly higher ionic conductivity than the base electrolyte due to the increase in the number of free ions arising

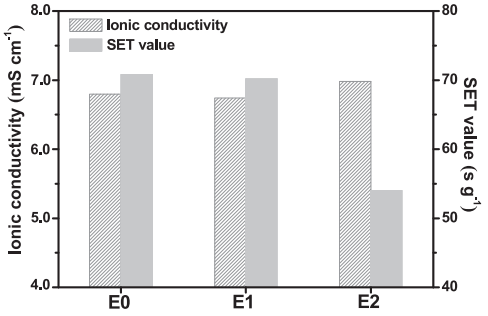

Fig. 1. Ionic conductivities and SET values of different electrolyte systems.

from the dissociation of TEMEP-TFSI surpassing the decrease of the ionic mobility in the electrolyte solution. In order to investigate the flammable behavior of the electrolyte solution containing non-flammable ionic liquid, TEMEP-TFSI, flammability tests were performed. When TEMEP-TFSI was added to the electrolyte, both the burning time and flame intensity decreased, resulting in reduced flammability. Accordingly, the SET values of the electrolyte solution containing TEMEP-TFSI (E2) decreased. As previously reported [23,24], the flammability of an electrolyte solution is proportional to the SET value. Thus, this result suggests that the addition of a small amount of TEMEP-TFSI to the base electrolyte is effective in reducing the flammability of the electrolyte.

Fig. 2 shows the charge and discharge curves of $Li/LiMn_{1.5}Ni_{0.5}O_4$ cells with different electrolyte solutions for the first and second preconditioning cycles, which are obtained at a constant current rate of 0.1 C. It is well known that the SEI film formed in the preconditioning cycles can prevent the electrolyte from degradation for subsequent cycling, and thus improve cycling stability. In order to effectively form SEI film on the electrode surface, the current density was kept to be low (0.1 C rate) in the preconditioning cycles. As shown in Fig. 2, all the cells exhibited a voltage plateau near 4.7 V that is attributed to the Ni^{2+}/Ni^{4+} redox reaction and also a very small voltage plateau region of 4.0 V from the Mn^{3+}/Mn^{4+} redox process. For the base electrolyte, the first discharge capacity was 139.4 mAh g^{-1} based on active $LiMn_{1.5}Ni_{0.5}O_4$ material, a coulombic efficiency of 87.4%. The discharge capacity slightly decreased to 139.0 mAh g^{-1}, and the efficiency increased to 94.9% for the second cycle. The cells assembled with the E1 and E2 electrolytes exhibited reduced coulombic efficiencies of 82.9 and 79.4% at the first cycle for E1 and E2, respectively. This result may be explained by the irreversible electrochemical oxidation of DMAc and TEMEP-TFSI at high voltages during the first charging cycle, which leads to the formation of a solid electrolyte interphase (SEI) on the surface of the $LiMn_{1.5}Ni_{0.5}O_4$ electrode. At the second cycle, the coulombic efficiencies remarkably increased to 93.2 and 92.8% for E1 and E2, respectively. Higher efficiencies at the second cycle indicate that the oxidative decomposition of the electrolyte is suppressed by the SEI layer formed at the first cycle. The aluminum foil used as the positive current collector was not corroded by TFSI anion at high voltages during cycling, because the amount of TEMEP-TFSI was quite low as compared to $LiPF_6$ salt. Recently, Cho et al. have reported that the addition of a small amount of $LiPF_6$ in ionic liquid electrolyte containing TFSI anion led to inhibition of Al corrosion [25].

The cycling performance of the $Li/LiMn_{1.5}Ni_{0.5}O_4$ cells assembled with different electrolyte solutions was evaluated. After two preconditioning cycles at the 0.1 C rate, the cells were charged at 0.5 C rate up to a set voltage of 4.9 V, followed by a constant voltage charge until the final current reached 10% of the charging current. The cells were then discharged down to a cut-off voltage of 3.0 V at the same current (0.5 C). Fig. 3 shows the discharge capacities as a function of the cycle number in the cells prepared with

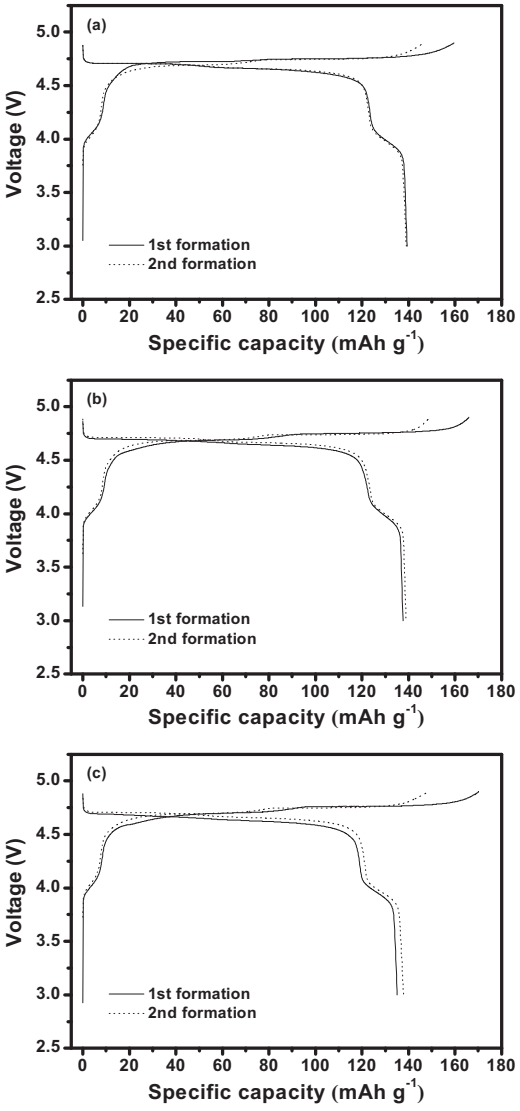

Fig. 2. Initial preconditioning charge-discharge curves of Li/$LiMn_{1.5}Ni_{0.5}O_4$ cells assembled with different electrolytes (current rate: 0.1 C, cut-off: 3.0–4.9 V, 25 °C) (a) E0, (b) E1 and (c) E2.

different electrolytes. The initial discharge capacity was nearly the same, irrespective of the type of the electrolyte, but the cycling stability of the cells is dependent on the type of electrolyte solution. With respect to the capacity retention, the cell with

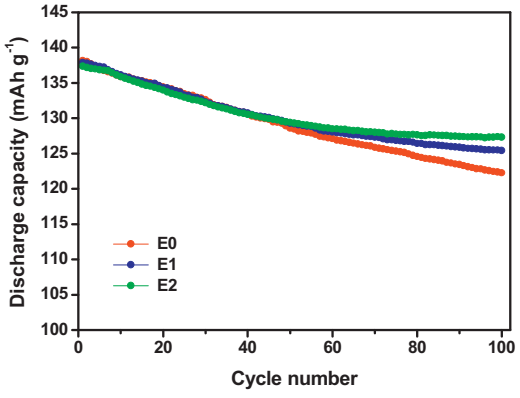

Fig. 3. Discharge capacities as a function of the cycle number for Li/$LiMn_{1.5}Ni_{0.5}O_4$ cells assembled with the different electrolytes (0.5 C CC and CV charge, 0.5 C CC discharge, cut-off voltage range: 3.0–4.9 V, 25 °C).

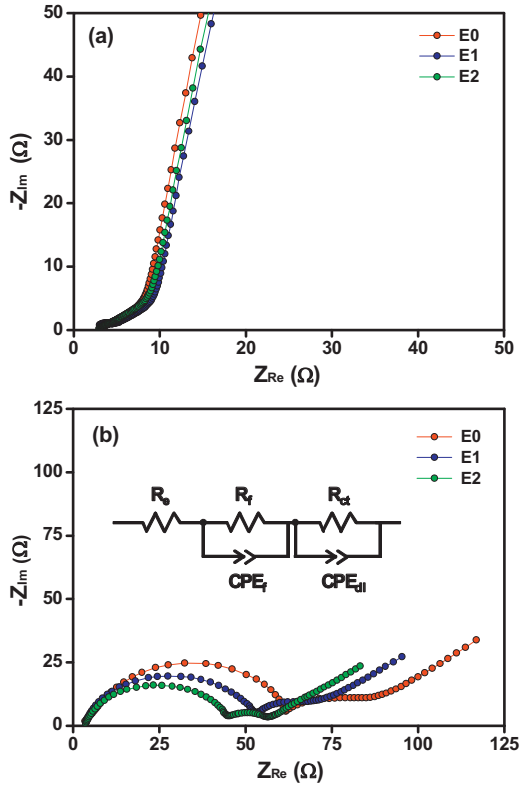

Fig. 4. AC impedance spectra of Li/$LiMn_{1.5}Ni_{0.5}O_4$ cells assembled with different electrolytes (a) before and (b) after 100 cycles.

the E2 electrolyte exhibited the most stable cycling behavior, maintaining 92.6% of its initial discharge capacity after 100 cycles. Good capacity retention in the cell with the E2 electrolyte may be ascribed to the surface layer formed on the $LiMn_{1.5}Ni_{0.5}O_4$ electrode during the preconditioning cycles, which inhibits direct contact of the electrolyte with the $LiMn_{1.5}Ni_{0.5}O_4$ electrode and thus reduces the oxidative decomposition of the electrolyte on the electrode at high voltages.

In order to investigate the effect of the addition of DMAc and TEMEP-TFSI on the cycling performance, the AC impedance of the cells before and after repeated cycles (100 cycles) was measured, and the resultant AC impedance spectra are shown in Fig. 4-(a) and (b), respectively. Before cycling, the nearly identical AC impedance spectra indicate that the addition of DMAc and TEMEP-TFSI into the base electrolyte has no effect on the interfacial behavior of the cell before cycling. After charge and discharge cycling, two overlapping semicircles were observed, as shown in Fig. 4-(b). According to previous AC impedance studies [26–28], the semicircle in the high frequency range is associated with the surface film resistance on the electrode (R_f), while the semicircle observed in the medium-to-low frequency range is ascribed to the charge transfer resistance between the electrode and electrolyte (R_{ct}). These spectra could be analyzed by using the equivalent circuit given in the inset of Fig. 4-(b). In this circuit, R_e is the electrolyte resistance and corresponds to the high frequency intercept at the real axis. R_f and R_{ct} are the resistance of Li^+ ions through SEI film and the charge transfer resistance, respectively. CPE_i (constant phase element) denotes the capacitance of each component to reflect the depressed semi-circular shape. The cell assembled with the E2 electrolyte showed the lowest surface film resistance and charge transfer resistance. This result indicates that the addition of TEMEP-TFSI has a beneficial influence on the formation of a less-resistive SEI layer on the electrode and a facile charge transfer reaction, which is similar to the results of the metal oxide coating of the $LiMn_{1.5}Ni_{0.5}O_4$

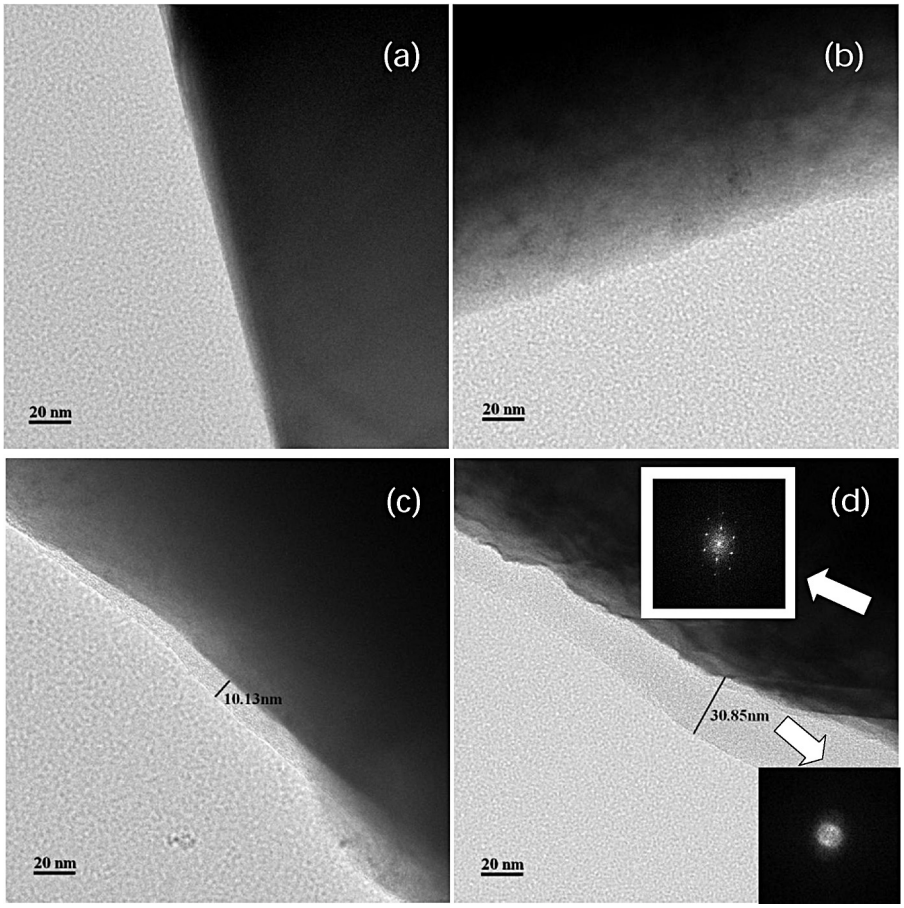

Fig. 5. TEM images of $LiMn_{1.5}Ni_{0.5}O_4$ cathode active materials before and after 100 cycles in different electrolytes: (a) pristine $LiMn_{1.5}Ni_{0.5}O_4$ electrode and $LiMn_{1.5}Ni_{0.5}O_4$ electrodes cycled in (b) E0, (c) E1 and (d) E2.

electrode that suppressed the increase in impedance of the cell during cycling, leading to good capacity retention [12–14].

To clarify the effect of the additives on the formation of the SEI layer on the $LiNi_{0.5}Mn_{1.5}O_4$ cathode material, the surface of the $LiNi_{0.5}Mn_{1.5}O_4$ particle was analyzed by TEM. Fig. 5 shows the high resolution TEM images of the pristine $LiNi_{0.5}Mn_{1.5}O_4$ particle and $LiNi_{0.5}Mn_{1.5}O_4$ particles cycled in different electrolytes. The pristine $LiNi_{0.5}Mn_{1.5}O_4$ particle does not have an extra film on the particle surface. Alternatively, the magnified images around the edge of the $LiNi_{0.5}Mn_{1.5}O_4$ particles cycled in E1 and E2 reveal a thin layer ranging from 10 to 31 nm. The thickness is greater in the $LiNi_{0.5}Mn_{1.5}O_4$ electrode cycled in E2 compared to that in E1. Accordingly, the improved cycling performance in the E2 electrolyte can be ascribed to the formation of a protective surface layer, which inhibits the harmful interfacial side reactions between the $LiNi_{0.5}Mn_{1.5}O_4$ electrode and electrolyte. The selected area electron diffraction (SAED) patterns obtained from the particle (black part) and surface layer (gray part) on the $LiNi_{0.5}Mn_{1.5}O_4$ particle cycled in E2 are also shown in the insets of Fig. 5. The SAED pattern from the $LiNi_{0.5}Mn_{1.5}O_4$ particle is quite different from one in the surface layer, indicating that the $LiNi_{0.5}Mn_{1.5}O_4$ particle is covered with the surface layer composed of different compounds.

In order to identify the chemical species formed on the surface of $LiNi_{0.5}Mn_{1.5}O_4$ electrodes cycled in different electrolytes, the XPS measurements were performed after 100 cycles. As shown in Fig. 6, the XPS analysis of the electrode surface reveals significant differences in the surface species. Compared to the pristine $LiNi_{0.5}Mn_{1.5}O_4$ electrode, the concentrations of C, Ni, and Mn decreased for cycled $LiNi_{0.5}Mn_{1.5}O_4$ electrodes, while the concentrations of O, F, and P increased, indicating that the $LiNi_{0.5}Mn_{1.5}O_4$ electrode is covered by the surface layer. The C1s spectrum of the electrode cycled in the base electrolyte (E0) shows four peaks, which are hydrocarbons (C-H, C-C at 284.6 eV), C-O-C bonds (286-287 eV), C=O bonds (288.5 eV) and C-F_2 from PVdF (291 eV) [16,29]. A noticeable feature for the electrodes cycled in E1 or E2 is the appearance of a C-N peak at 286.3 eV [30,31], which arises from the decomposition product of DMAc or the TFSI anion in the ionic liquid. The O1s spectrum in the base electrolyte exhibits three main peaks, C-O bonds (533.7 eV), C=O bonds (532.1 eV), and the $LiNi_{0.5}Mn_{1.5}O_4$ peak (529.8 eV). However, the peak corresponding to $LiNi_{0.5}Mn_{1.5}O_4$ is not observed in the electrodes cycled in the E1 or E2 electrolyte, which suggests that cycling causes the $LiNi_{0.5}Mn_{1.5}O_4$ electrode to be fully covered with a surface layer, as shown in Figs. 5-(c) and (d). The F1s spectrum in the base electrolyte is composed of C-F_2 from PVdF (687.9 eV), $Li_xPO_yF_z$ (686.2 eV) and LiF (685.0 eV) [31,32]. In E1 and E2 electrolytes, the LiF intensity is weaker than that of electrode cycled in E0. Moreover, the $Li_xPO_yF_z$ peak is hardly observed in the E1 and E2 electrolytes. The formation of resistive layers on the $LiNi_{0.5}Mn_{1.5}O_4$ surface is closely associated with the decomposition of $LiPF_6$ [33,34]. LiF and $Li_xPO_yF_z$ are decomposition products of $LiPF_6$ which tend to easily precipitate on the surface of the cathode active materials and thus act as resistive layers for retarding charge transport. Therefore, the byproducts deposited on the $LiNi_{0.5}Mn_{1.5}O_4$ surface are likely to be crucial for high interfacial resistances (i.e., R_f and R_{ct}) in E0. A new peak at 689.5 eV, characteristic of the C-F_x peak, is observed in E2 electrolyte [30], indicating the TFSI anion in the ionic liquid decomposes to form the surface film on the $LiNi_{0.5}Mn_{1.5}O_4$ electrode. These results suggest that the oxidative decomposition of TEMEP-TFSI occurs on the $LiNi_{0.5}Mn_{1.5}O_4$ electrode surface before

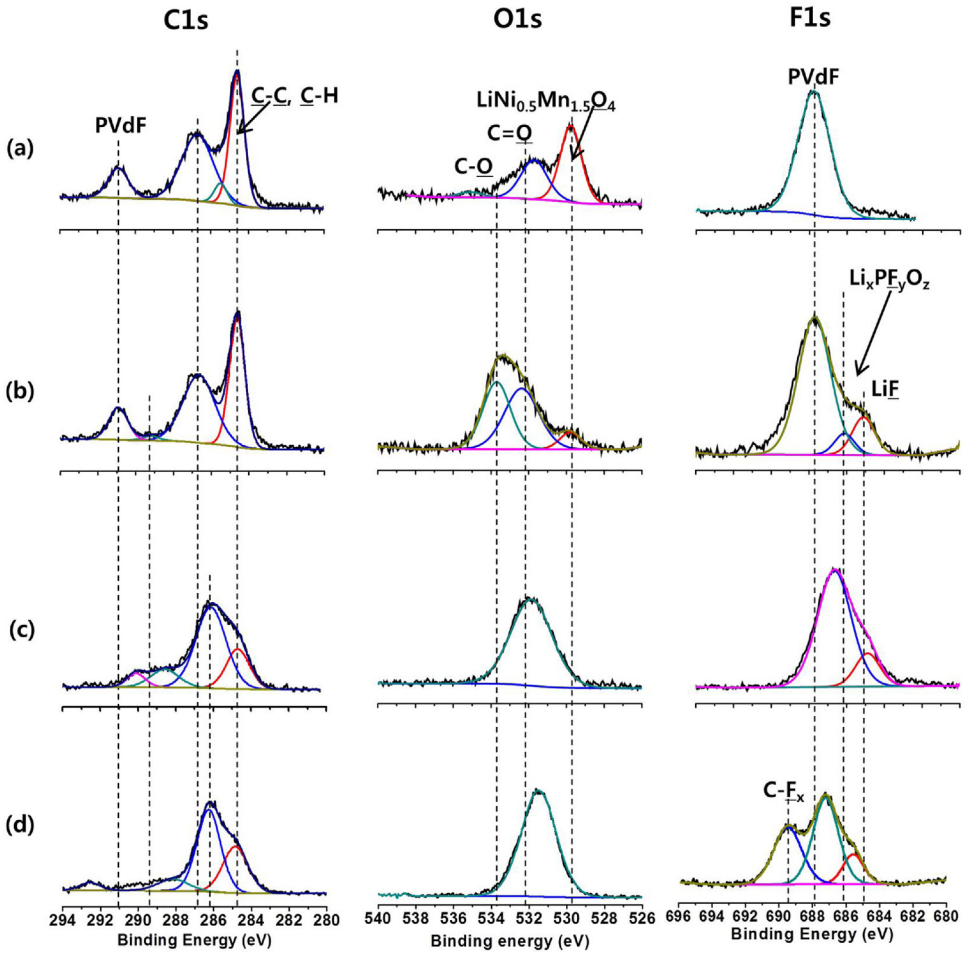

Fig. 6. XPS spectra of $LiMn_{1.5}Ni_{0.5}O_4$ electrodes before and after 100 cycles in different electrolytes: (a) pristine $LiMn_{1.5}Ni_{0.5}O_4$ electrode and $LiMn_{1.5}Ni_{0.5}O_4$ electrodes cycled in (b) E0, (c) E1 and (d) E2.

other components in the electrolyte, and the resulting surface layer effectively mitigates the electrolyte decomposition.

The thermal stability of delithiated $Li_{1-x}Ni_{0.5}M_{1.5}O_4$ materials in the presence of different electrolyte solutions was evaluated. Fig. 7 compares the DSC profiles of the charged cathode materials after 100 cycles. The thermal stability of $Li_{1-x}Ni_{0.5}M_{1.5}O_4$ materials is affected by the type of electrolyte solution. The overall exothermic heat generated by the thermal reaction of the charged cathode is 60.4 and 22.3 J g^{-1} for E1 and E2, respectively, which are much lower than that measured in the base liquid electrolyte (217.4 J g^{-1}). Moreover, the onset temperature of the exothermic reactions increased with the addition of a small amount of TEMEP-TFSI. These results suggest that the charged $LiNi_{0.5}M_{1.5}O_4$ material is less reactive toward the electrolyte solution containing an ionic liquid, leading to improved thermal stability. This result also reflects that the surface layer formed on the cathode materials in the E2 electrolyte rendered the cathode materials less reactive toward the electrolyte solution.

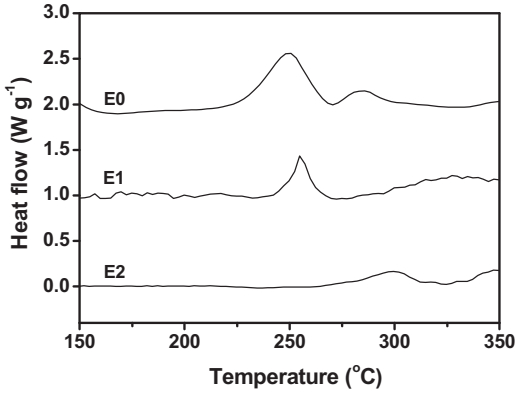

Fig. 7. DSC profiles of the $LiMn_{1.5}Ni_{0.5}O_4$ cathode materials charged to 4.9 V after 100 cycles in the cells assembled with different electrolytes.

4. Conclusions

Non-flammable ionic liquid, TEMEP-TFSI as well as DMAc, were investigated as protective film-forming additives to improve the thermal stability and cycling performance of high-voltage spinel $LiNi_{0.5}M_{1.5}O_4$ electrode. The addition of these additives into the base electrolyte improved the capacity retention and reduced the flammability of the electrolyte solution. The surface analysis of the $LiNi_{0.5}M_{1.5}O_4$ electrode after cycling showed that the additives could form a stable surface layer on $LiNi_{0.5}M_{1.5}O_4$, which suppressed the electrolyte decomposition during cycling. The DSC results revealed that the addition of TEMEP-TFSI significantly improved the thermal stability of the charged $LiNi_{0.5}M_{1.5}O_4$ electrode.

Acknowledgement

This work was supported by the IT R&D program of MKE/KEIT (KI002176-2010-02) and by a grant from the National Research

Foundation of Korea funded by the MEST of the Korean Government (NRF-2009-C1AAA001-0093307)

References

[1] J.H. Kim, S.T. Myung, Y.K. Sun, Molten salt synthesis of $LiNi_{0.5}Mn_{1.5}O_4$ spinel for 5 V class cathode material of Li-ion secondary battery, Electrochim. Acta 49 (2004) 219.

[2] T.-F. Yi, Y.-R. Zhu, R.-S. Zhu, Density functional theory study of lithium intercalation for 5 V $LiNi_{0.5}Mn_{1.5}O_4$ cathode materials, Solid State Ionics 179 (2008) 2132.

[3] Y. Sun, Y. Yang, H. Zhan, H. Shao, Y. Zhou, Synthesis of high power type $LiMn_{1.5}Ni_{0.5}O_4$ by optimizing its preparation conditions, J. Power Sources 195 (2010) 4322.

[4] M. Ue, K. Ida, S. Mori, Electrochemical properties of organic liquid electrolytes based on quaternary onium salts for electrical double-layer capacitors, J. Electrochem. Soc. 141 (1994) 2989.

[5] H. Lee, S. Choi, S. Choi, H.J. Kim, Y. Choi, S. Yoon, J.J. Cho, SEI layer-forming additives for $LiNi_{0.5}Mn_{1.5}O_4$/graphite 5 V Li-ion batteries, Electrochem. Commun. 9 (2007) 801.

[6] R. Mogi, M. Inaba, S. Jeong, Y. Iriyama, T. Abe, Z. Ogumi, Effects of some organic additives on lithium deposition in propylene carbonate, J. Electrochem. Soc. 149 (2002) 1047.

[7] H. Ota, K. Shima, M. Ue, J. Yamaki, Effect of vinylene carbonate as additive to electrolyte for lithium metal anode, Electrochim. Acta 49 (2004) 565.

[8] M. Ishikawa, H. Kawasaki, N. Yoshimoto, M. Morita, Pretreatment of Li metal anode with electrolyte additive for enhancing Li cycleability, J. Power Sources 146 (2005) 199.

[9] K. Abe, Y. Ushigoe, H. Yoshitake, M. Yoshio, Functional electrolytes: Novel type additives for cathode materials, providing high cycleability performance, J. Power Sources 153 (2006) 328.

[10] K.S. Lee, Y.K. Sun, J. Noh, K.S. Song, D.W. Kim, Improvement of high voltage cycling performance and thermal stability of lithium-ion cells by use of a thiophene additive, Electrochem. Commun. 11 (2009) 1900.

[11] Y.S. Lee, K.S. Lee, Y.K. Sun, Y.M. Lee, D.W. Kim, Effect of an organic additive on the cycling performance and thermal stability of lithium-ion cells assembled with carbon anode and $LiNi_{1/3}Co_{1/3}Mn_{1/3}O_2$ cathode, J. Power Sources 196 (2011) 6997.

[12] Y.K. Sun, K.J. Hong, J. Prakash, K. Amine, Electrochemical performance of nano-sized ZnO-coated $LiNi_{0.5}Mn_{1.5}O_4$ spinel as 5 V materials at elevated temperatures, Electrochem. Commun. 4 (2002) 344.

[13] Y. Kobayashi, H. Miyashiro, K. Takei, H. Shigemura, M. Tabuchi, H. Kageyama, T. Iwahori, 5 V class all-solid-state composite lithium battery with Li_3PO_4 coated $LiNi_{0.5}Mn_{1.5}O_4$, J. Electrochem. Soc. 150 (2003) A1577.

[14] R. Alcantara, M. Jaraba, P. Lavela, J.L. Tirado, X-ray diffraction and electrochemical impedance spectroscopy study of zinc coated $LiNi_{0.5}Mn_{1.5}O_4$ electrodes, J. Electroanal. Chem. 566 (2004) 187.

[15] S. Santee, A. Xiao, L. Yang, J. Gnanaraj, B.L. Lucht, Effect of combinations of additives on the performance of lithium ion batteries, J. Power Sources 194 (2009) 1053.

[16] M. Xu, L. Hao, Y. Liu, W. Li, L. Xing, B. Li, Experimental and theoretical investigations of dimethylacetamide (DMAc) as electrolyte stabilizing additive for lithium ion batteries, J. Phys. Chem. C 115 (2011) 6085.

[17] M. Galinski, A. Lewandowski, I. Stepniak, Ionic liquids as electrolytes, Electrochim. Acta 51 (2006) 5567.

[18] M. Armand, F. Endres, D.R. MacFarlane, H. Ohno, B. Scrosati, Ionic-liquid materials for the electrochemical challenges of the future, Nature Mater. 9 (2009) 621.

[19] J.A. Choi, Y.K. Sun, E.G. Shim, B. Scrosati, D.W. Kim, Effect of 1-butyl-1-methylpyrrolidinium hexafluorophosphate as a flame-retarding additive on the cycling performance and thermal properties of lithium-ion batteries, Electrochim. Acta 56 (2011) 10179.

[20] K. Tsunashima, M. Sugiya, Physical and electrochemical properties of low-viscosity phosphonium ionic liquids as potential electrolytes, Electrochem. Commun. 9 (2007) 2353.

[21] S.M. Eo, E. Cha, D.W. Kim, Effect of an inorganic additive on the cycling performances of lithium-ion polymer cells assembled with polymer-coated separators, J. Power Sources 189 (2009) 766.

[22] D. Zhou, W. Li, C. Tan, X. Zuo, Y. Huang, Cresyl diphenyl phosphate as flame retardant additive for lithium-ion batteries, J. Power Sources 184 (2008) 589.

[23] K. Xu, M.S. Ding, S. Zhang, J.L. Allen, T.R. Jow, An attempt to formulate non-flammable lithium ion electrolytes with alkyl phosphates and phosphazenes, J. Electrochem. Soc. 149 (2002) A622.

[24] S.R. Sivakkumar, D.R. MacFarlane, M. Forsyth, D.W. Kim, Ionic liquid-based rechargeable lithium metal-polymer cells assembled with polyaniline/carbon nanotube composite cathode, J. Electrochem.Soc. 154 (2007) A834.

[25] E. Cho, J. Mun, O.B. Chae, O.M. Kwon, H.T. Kim, J.H. Ryu, Y.G. Kim, S.M. Oh, Corrosion/passivation of aluminum current collector in bis(fluorosulfonyl) imide-based ionic liquid for lithium-ion batteries, Electrochem. Commun. 22 (2012) 1.

[26] A. Funabiki, M. Inaba, Z. Ogumi, AC impedance analysis of electrochemical lithium intercalation into highly oriented pyrolytic graphite, J. Power Sources 68 (1997) 227.

[27] M.D. Levi, G. Salitra, B. Markovsky, H. Teller, D. Aurbach, U. Heider, L. Heider, Solid-state electrochemical kinetics of Li-ion intercalation into $Li_{1-x}CoO_2$: simultaneous application of electroanalytical techniques SSCV, PITT and EIS, J. Electrochem. Soc. 146 (1999) 1279.

[28] J.M. Zheng, Z.R. Zhang, X.B. Wu, Z.X. Dong, Z. Zhu, Y. Yang, The effects of AlF_3 coating on the performance of $Li[Li_{0.2}Mn_{0.54}Ni_{0.13}Co_{0.13}]O_2$ positive electrode material for lithium-ion battery, J. Electrochem.Soc. 155 (2008) A775.

[29] S.Y. Ha, J.G. Han, Y.M. Song, M.J. Chun, S.I. Han, W.C. Shin, N.S. Choi, Using a lithium bis(oxalato) borate additive to improve electrochemical performance of high-voltage spinel $LiNi_{0.5}Mn_{1.5}O_4$ cathodes at 60 (C, Electrochim. Acta 104 (2013) 170.

[30] T. Sugimoto, M. Kikuta, Ionic liquid electrolytes compatible with graphitized carbon negative without additive and their effects on interfacial properties, J. of Power Sources 183 (2008) 436.

[31] J. Mun, S. Kim, T. Yim, J.H. Ryu, Y.G. Kim, S.M. Oh, Comparative study on surface films from ionic liquids containing saturated and unsaturated substituent for $LiCoO_2$, J. Electrochem. Soc. 157 (2010) A136.

[32] Li. Yang, B.L. Lucht, Inhibition of electrolyte oxidation in lithium ion batteries with electrolyte additives, Electrochem. Solid-State Lett. 12 (2009) A229.

[33] J. Liu, A. Manthiram, Improved electrochemical performance of the 5 V spinel cathode $LiMn_{1.5}Ni_{0.42}Zn_{0.08}O_4$ by surface modification, J. Electrochem. Soc. 156 (2009) A66.

[34] H. Deng, I. Belharouak, C.S. Yoon, Y.K. Sun, K. Amine, High temperature performance of surface-treated $Li_{1.1}(Ni_{0.15}Co_{0.1}Mn_{0.55})O_{1.95}$ layered oxide, J. Electrochem. Soc. 157 (2010) A1035.